Edmond P. Saliklis,[1] *Steven M. Cramer,*[2] *and John C. Hermanson*[3]

Measuring the Triaxial Load-Deformation Response of Orthotropic Materials Subjected to Large and Small Strain Regimes

REFERENCE: Saliklis, E. P., Cramer, S. M., and Hermanson, J. C., **"Measuring the Triaxial Load-Deformation Response of Orthotropic Materials** Subjected **to Large and Small Strain Regimes,"** *Journal of Testing and Evaluation,* JTEVA, Vol. 26, No. 5, September 1998, pp. 444–454.

ABSTRACT: A new method for obtaining triaxial stress versus strain data is presented. The method tests cubic specimens and can provide constitutive data along three mutually perpendicular axes. Issues of removing the effects of boundary conditions in the proposed device are discussed. Two devices were constructed and used to obtain triaxial stress versus strain data on paperboard and on redwood samples. Representative data are shown.

KEYWORDS: triaxial testing, orthotropic materials, paperboard, redwood, surface effects

Paperboard and wood have traditionally been modeled as orthotropic elastic solids for advanced stress analysis. Such assumptions of orthotropicity have traditionally called for a constitutive model in the form of Hooke's law. An inherent weakness of this constitutive model is its limitation to the linear elastic regime of material response. Currently there is no generally accepted methodology of modifying this model to predict multiaxial material response beyond the linear range, although some researchers have proposed [*1*] and utilized [*2,3*] nonlinear biaxial theories. Additionally, the orthotropic form of Hooke's law has not been experimentally verified for these materials, except for a relatively small number of uniaxial and biaxial tests [*4,5*]. Although measurements of elastic constants have been the subject of some studies [*6,7*], in a review of the literature we found no published studies that have measured the triaxial response of paperboard or wood subjected to small and large strains. As the use of finite element analysis in design of products subjected to multiaxial stress states becomes more routine, it is important to re-examine and verify the material modeling assumptions employed. In this investigation, we attempted to better characterize paperboard and wood for packaging designs.

This paper presents a new method for obtaining experimental triaxial stress versus strain data from cubic specimens. We present two approaches for measuring the triaxial load-deformation response of paperboard and wood. The experimental details and design concepts characterize the use of new devices. Both experimental devices use a combination of actively and passively loaded axes. The goal of gathering triaxial load-deformation data is to transform this information into stresses and strains, so that the constitutive relationship mapping stresses into strains can be established empirically or new theoretical formulations can be evaluated.

The difficulties of measuring triaxial load-deformation response of orthotropic materials are also discussed. With any test device, isolating the material response is always obstructed by boundary conditions that occur at the surface of the specimen. Multiaxial experimental work will always require efforts to minimize surface effects as well as account for the surface effects that unavoidably remain. Another difficulty is that large displacements of the deformed specimen can significantly alter the resultant of the restraining forces, because the final geometry of the specimen can be markedly different than its original geometry. An issue related to the experimental design of the devices presented here is that the stress-strain paths are determined by the Poisson response of the material and cannot be chosen arbitrarily. All of these difficulties were addressed, and corrective measures are proposed for the specific experimental methods and devices described here.

General Approach

An orthotropic material is one with three orthogonal planes of material property symmetry. Thus, measurement of orthotropic response requires load and deformation measurement along three mutually perpendicular axes. Our general approach consisted of active loading in compression along one axis and passive loading along the two normal axes by restricting lateral expansion. The passive restraint system offered by the confining box avoids the need for a complex hydraulic setup with multiple actuators. Lateral restraint is provided by a rigid confining box (Figs. 1 and 2.) Although this design imposes some experimental challenges (which were subsequently addressed), it was chosen in preference to a cylindrical type of triaxial test such as ASTM Standard C801: Test Method for Performing the Mechanical Properties of Hardened Concrete Under Triaxial Loads [*8*] in order to acquire orthogonal data to define behavior along the three principal axes. To achieve known boundary conditions, it is desirable to apply the loads as uniformly as possible over the specimen surfaces. Thus, the confining box must fit precisely around the specimen. By this same reasoning, it is difficult to apply load actively in two or three directions through large deformations, which further supports our approach.

Manuscript received 03/11/96; accepted for publication 02/12/98.

[1] Formerly at USDA Forest Service, Forest Products Laboratory, Madison, WI. Currently at the Department of Civil and Environmental Engineering, Lafayette College, Easton, PA 18042.

[2] Department of Civil and Environmental Engineering, University of Wisconsin, Madison, WI 53705.

[3] Wood Materials and Engineering Lab, Washington State University, Pullman, WA 99164.

© 1998 by the American Society for Testing and Materials

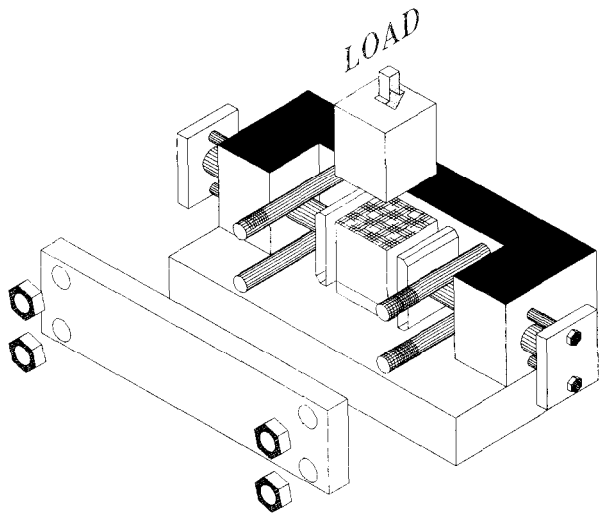

FIG. 1—*Paperboard testing device.*

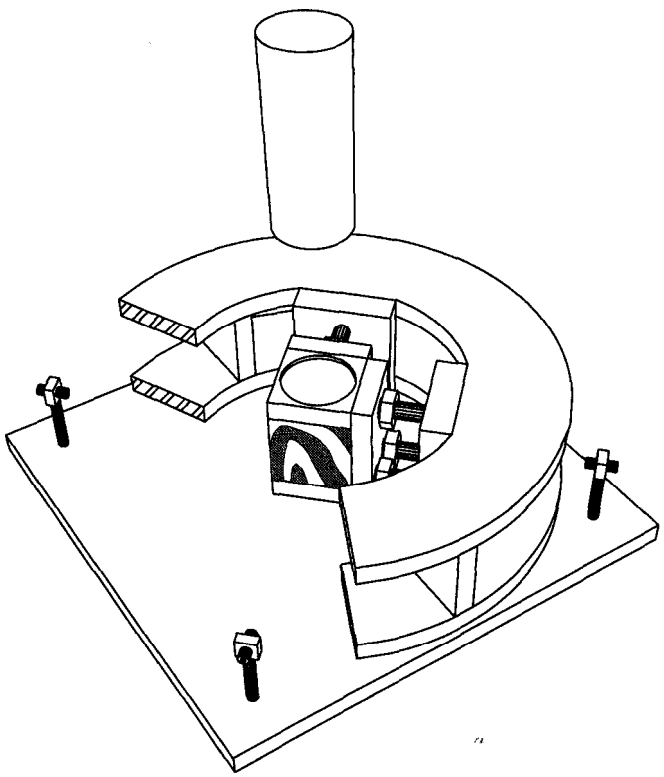

FIG. 2—*Redwood testing device.*

An inherent difficulty of the passive restraint system is that the stress-strain history of a test must follow a fixed path. For a given specimen orientation and axial load, only one transverse load combination is possible. The amount of compressive force built up by the restraining transverse axes is a function of the force in the active loading direction and the Poisson effect relating the two axes. This experimental constraint was minimized by utilizing all possible specimen orientations in the triaxial testing device to derive a single constitutive model. The actively loaded orientations were physically changed from test to test. Combining this information with classical transformation formulas allowed a general collection of triaxial data.

Orthotropic Test Materials

The paperboard specimens were composite materials constructed of layers of paper and silicate adhesive. Paper sheets have three principal directions: (1) machine direction (MD), along which the majority of wood fibers are aligned; (2) cross direction (CD), which is 90° to MD in the plane of the paper; and (3) Z direction (ZD), which is normal to the plane of the paper. Since each sheet was aligned squarely as the specimen was laid up, the resultant composite had these three principal directions. During the testing program, seven batches of paperboard laminates were fabricated from a single grade of paper. Cubes (32 mm on each side) were cut from sheets of the composite paperboard material. Specimen size and the resulting test device size were limited by the difficulty in laminating paperboard stock into composite sheets thicker than 32 mm. Typical moduli for the specimens were E_{MD} = 6800 MPa, E_{CD} = 2700 MPa, and E_{ZD} = 90 MPa.

The wood specimens were solid 100-mm cubes, cut and machined from eight commercially obtained, standard 140- by 140-mm (nominal 6- by 6-in.) redwood timbers. Stock was selected on the basis of straightness of grain, lack of knots, specific gravity, and number of annual growth rings. For the redwood testing program, we gathered extensive data on crushing of specimens at various grain angles. Specimens were fabricated from timber stock for target fiber angles of 0°, 5°, 10°, 30°, and 90°. Because of the size limitations associated with the nominal sizes of stock timbers, specimens with fiber angles between 30° and 90° could not be extracted. Final grain angles were established within ± 1° using an electronic scanner. Whereas the paperboard testing device was designed to investigate response in only the principal material directions, the redwood testing device was designed to investigate off-axis response as well. This necessitated a change in the lateral support system (discussed later). Typical moduli for the redwood specimens were E_L = 9700 MPa, E_R = 830 MPa, and E_T = 90 MPa, where L refers to longitudinal direction and R and T to radial and tangential directions, respectively.

Triaxial Testing Devices

In both testing devices, the hydraulic axial testing machine actively loaded one axis of the specimen, while the two transverse axes were restrained from free expansion by the mechanisms shown in Figs. 1 and 2. Vertical displacement was monitored by internal stroke measurements of the testing machine in the paperboard testing device and a linear variable differential transformer (LVDT) placed on the loading head of the redwood testing device. The general principle common to both devices is that triaxial stress is incurred by using a confining box of steel with adjustable platens attached by bolts (see Figs. 1 and 2). The loads and deformations were monitored on all three orthogonal axes. In both devices, strain gages were mounted on the lateral restraining bolts in a Wheatstone bridge circuit to determine the lateral load. In the paperboard testing device, deformations were inferred from loads through a predetermined load-displacement curve for each component of the restraining mechanisms on the two passive axes. Each load-carrying bolt was manually tightened after the specimen was placed within the device so that a small initial pressure was present, approximately 0.137 MPa. Platens on the transverse axes were polished stainless-steel-coated plates. The restraining force was assumed to be normal to the specimen surface throughout the test because the strain on these transverse axes was small, on the order of 0.001 mm/mm. The deformations in the active loading direction

were directly measured by the axial testing machine, and they could result in strain as great as 0.08 to 0.10 mm/mm. The confining box design did not allow for measurements of deformations other than those at the specimen surfaces.

A second confining box was designed to test redwood; the box was modified to reflect different experimental conditions and our experience gained from the paperboard testing device. Figure 2 shows the test device in perspective view. A 100-mm redwood cube was confined by loading platens, load bolts, bolt support plates, reaction ring, and reaction ring base plate. This new ring design was chosen to create symmetrical restraint conditions and independent load- and deflection-measuring systems. The confining ring was sized to allow no more than 0.051 mm of total lateral expansion. Sockets were bored into the lateral plates to accept 25-mm-diameter stainless steel balls to transfer the loads from the platens to the bolts. In both devices, the lateral loads exerted by the specimen on the test device were measured by strain gages mounted on the bolts supporting the lateral platens. However, in the redwood testing device, the A325 structural bolts served several functions in the overall design. In addition to acting as load transducers, bolt positioning was accommodated by the threads, which allowed for a precise fit of the lateral platens against the orthotropic specimens.

A major design factor of the redwood testing device was that specimens were subject to crush strains as great as 75%. This amount of strain caused the resultant transverse forces to move vertically during the course of a test as the specimen was crushed. Many commercially available load cells were unable to accommodate the large moment caused by the resultant force. The strain-gaged bolts, arranged in a triangle, proved effective in measuring lateral loads and recording the moving location of the resultant force. The bolt load-indicating capability was calibrated to an error of less than 1% of the indicated load and provided a resolution of 13 N. Each bolt was designed to accommodate 111 200 N of total load.

Displacement-measuring capabilities of the redwood testing device were improved by threading an LVDT rod into the center of each lateral platen to measure its lateral displacement relative to the base plate. This was preferable to the previous design, which required an inference of lateral displacements based on the predetermined load-deformation history of the restraining bolts. Lateral displacements on the redwood testing device were measured with an accuracy of 0.0025 mm. Although generally restricted by the design of the restraining ring, small lateral deformations were unavoidable.

Surface Effects

An ideal triaxial test would allow simple and direct calculation of specimen stress and strain states solely from the acquired lateral load and deflection measurements. Such an ideal test would be minimally influenced by boundary and surface effects, and it would achieve a uniform stress and strain distribution throughout the specimen. In reality, this situation is nearly impossible to achieve because surface effects are always present along the boundaries of the specimen. Two separate surface effects must be accounted for when gathering data from devices such as the ones proposed here. The first surface effect comes from loading of the specimen surface, which introduces lateral frictional forces and creates a nonuniform strain distribution throughout the specimen. This nonuniform strain distribution results in a misleading determination of the material moduli. The second effect is crushing of local asperities at the metal-specimen interface. Wolcott et al. [*9*] suggested that such crushing of asperities could account for as much as a 50% error in moduli calculations.

One way to minimize surface effects is to have larger specimens, because the ratio of specimen surface area to specimen volume of a cube is $6/d$ (d = dimension). At the time of this test program, paperboard specimens were limited to 32 mm because of the lamination technique, resulting in a volume-to-surface area ratio of 5.3. The size of the wood cubic specimens was 100 mm so that various orientations of 90-mm (nominal 4-in.) cubes could be obtained from 140- by 140-mm (nominal 6- by 6-in.) redwood timber. This resulted in a more desirable volume-to-surface area ratio of 25.4. However, data from the redwood specimens were still influenced by frictional surface effects and surface asperities.

Several methods of analysis were used to quantify the surface effects. The goal was to account for the nonuniformity of strain distribution throughout the specimen, i.e., to remove such nonuniformities from the experimentally gathered load-deformation data. In the paperboard testing device, a finite element analysis of the effect of transverse frictional forces was conducted to quantify the frictional restraining forces of the stainless steel platens. Here, nonuniformity of strain distribution would be quantified if the modulus calculated from surface-to-surface strains differed from the modulus input into the finite element code. Eight-node solid-brick elements were used to model the specimen. The mesh was refined until the specimen was modeled by a 10 by 10 by 10 grid of solid elements, each element 3.2 mm on edge. In this model, the coefficient of friction was assumed infinitely large to see how great the effect was in the extreme case. Thus, fixed displacement boundary conditions were imposed in the x and y directions, transverse to the direction of loading (z direction) on the loaded surface of the specimen (Fig. 3). This model exhibits only transverse frictional forces on loaded surfaces (Fig. 3). The loading condition was a prescribed displacement on the top surface, to simulate more accurately the displacement-controlled uniaxial test. Deviations of input moduli from moduli calculated from loading surface-to-loading surface strains are solely a result of the nonuniform strain distribution caused by the surface frictional forces. Such a set of boundary conditions would actually increase the apparent moduli (read from loading platens) *if* the specimen aspect ratio (longitudinal/cross-sectional dimensions) was large, on the order of 5 to 10. However, for a cubical specimen like ours, the frictional forces oppose the poor geometry of the specimen and the net result is a lower apparent modulus read from the loading platens. These deviations were not great; the adjustment needed to bring the detected modulus to that of the finite element input was on the order of several percentage points (see Fig. 3).

In the redwood testing device, the coefficient of friction of the device-specimen interface was experimentally quantified. This value was then entered into a finite element analysis of the surface effect resulting from friction. This was a more rigorous quantification of the frictional effect than the simulation done on the paperboard device. Experiments were conducted to determine the test-specific coefficients of friction. These coefficients of friction ranged from 0.10 to 0.30 for the redwood specimens coated with paraffin wax, and from 0.30 to 0.60 for unwaxed specimens. These coefficients of friction were determined by measuring the force-displacement relationship of a specimen loaded along one axis and transversely restrained on an orthogonal axis. The loading rates for this friction test were approximately the same as that of the triaxial test, avoiding the need to distinguish static from dynamic coefficients of friction. All final triaxial tests were performed with wax-coated specimens to minimize frictional forces.

Local crushing of paperboard surface asperities was quantified through a series of uniaxial tests, which related platen movement

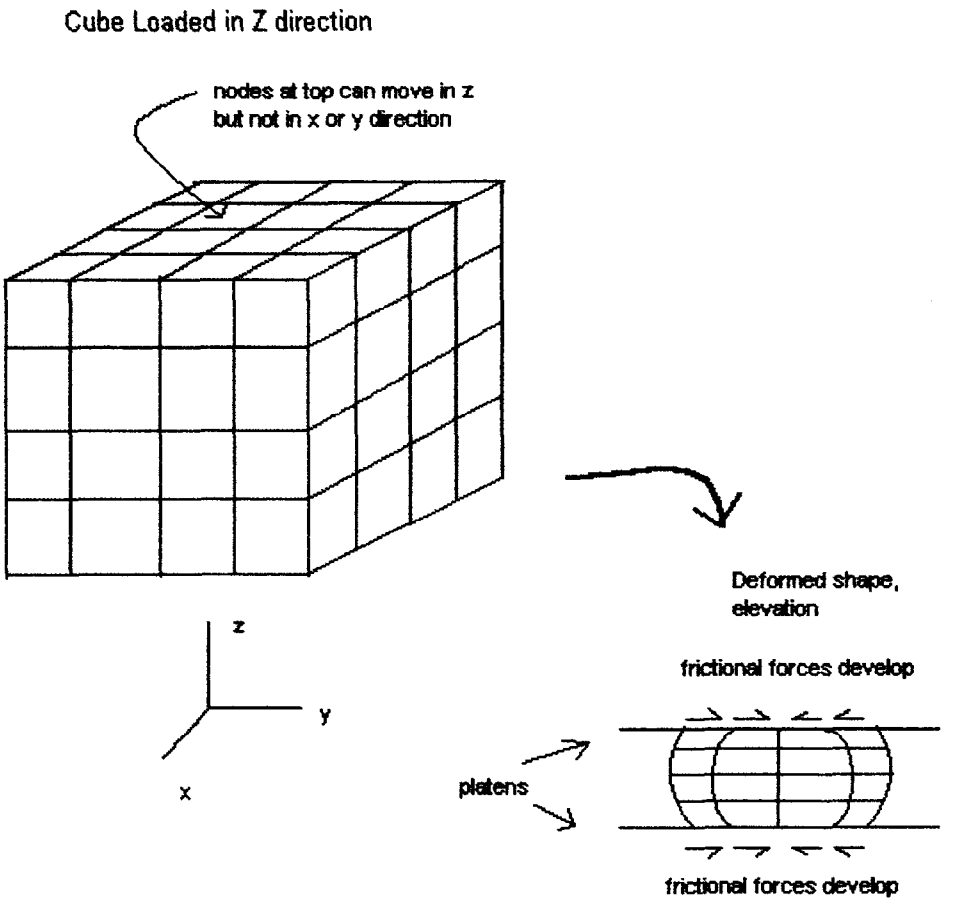

FIG. 3—*Frictional model using FEM.*

at the device-specimen interface to strain near the center of the specimen. Platen movement was easily measured by the head movement readings of the testing machine. The strain near the specimen was considered to be a more accurate indicator of the true material modulus. This center strain was measured by strain gages adhered to the specimen surface. Ideally, such gages would be present in a triaxial test as well, but this is not possible. The triaxial test is limited to platen movement readings only. Thus, it was necessary to quantify this difference of strain readings, which was caused by the surface effect of crushing of asperities. This effect was quite large (Fig. 4). Here, the detected modulus (read by platen movement) was only a fraction of the true material modulus (as indicated by strain gage readings near the center of the specimen). Furthermore, the initial portion of the test (low stresses) showed that almost all movement of the loading platen was due to local crushing. Only at higher stress levels did the platen (detected) reading closely resemble the gage reading, but even then it was approximately one third the gage (true) reading. This effect was most pronounced in the MD direction. The other two directions required much smaller adjustments.

Uniaxial tests accounting for local surface asperity crush of the redwood specimens gave similar results. The modulus of elasticity (E) detected from platen movement (surface-to-surface strain measurement) could be much lower than the true E measured by a centrally placed strain gage. Again, this effect was most pronounced in the stiffest direction, longitudinal (L), and less severe in the radial (R) and tangential (T) directions. Investigations of E for redwood are summarized in Table 1.

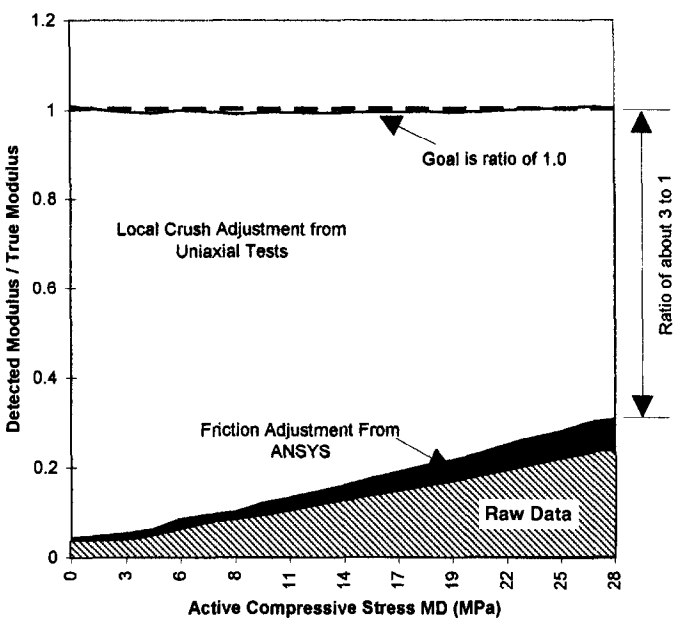

FIG. 4—*Adjustments for end effects in paperboard specimens (MD).*

Thus, it was necessary to account for the two surface effects and to adjust the moduli detected from loading-platen movement (see Fig. 4). To quantify these surface effects, we assumed that they were independent and uncoupled. This allowed us to investigate the effects as worst cases. It is unlikely that these effects could somehow interact to create more extreme, unaccounted-for surface effects. These adjustments allowed us to calculate the purported true mechanical response of the material.

Calibration of Test Devices

To validate the methodology of quantifying surface effects and to check the ability of the device to induce triaxial stress, a series of triaxial calibration tests were conducted with the paperboard testing device using polyethylene and acrylic isotropic specimens. However, before testing, adjustments for surface effects needed to be made, as described earlier. Thus, a finite element analysis was performed on each material to determine the effect of lateral restraint on the loading surfaces. The same mesh and element type was used for this analysis as for the paperboard analysis. Uniaxial tests were then performed on the polyethylene and acrylic specimens. As before, these tests included measurements of strain from platen movement compared to strain from a centrally placed strain gage. By combining these surface effects, we were then able to perform the triaxial test, with a resulting set of load-deflection data that accounted for the surface effects. The experimentally obtained stress versus strain responses of these two materials were verified by comparison to isotropic Hooke's law predictions. The agreement between the experimentally obtained and Hooke's law values validated the ability to quantify surface effects and gather triaxial data, within the linear regime.

All load and displacement transducers in the redwood testing device were calibrated prior to testing and met or exceeded accuracy limits set by ASTM Standard E4-94: Practice for Force Verification of Testing Machines [*10*]. The test data report [*11*] contains specific information on the calibration of all the equipment used. A final check on the calibration of the redwood testing device was performed using an aluminum block as the specimen. Details are found in the report [*11*].

TABLE 1—*Summary of measured redwood moduli.*

Modulus of Elasticity	Platen (Detected) Reading, MPa	Gage (True) Reading, MPa	Ratio (Detected/True)
E_L	2384	9239	0.26
E_R	299	775	0.39
E_T	196	267	0.73

Examples of Data

A total of 27 triaxial tests on paperboard were conducted, at – 5C° (± 1C°) and 50% (± 2%) relative humidity. Nine replications were performed in each principal direction (MD, CD, ZD). Tests were conducted under 0.08 to 0.10 mm/mm strain in the actively loaded direction. In the redwood testing program, 36 tests were conducted. Test strains reached as much as 75% in the actively loaded direction because both crush and lockup of redwood were investigated.

Figures 5 to 10 generally depict triaxial stresses and strains experienced by paperboard specimens. Figures 5, 7, and 9 show the scale of passive stresses (CD and ZD) formed when the active stress (MD) is applied. Figures 6, 8, and 10 depict the state of strain on the three orthogonal axes when load is actively applied

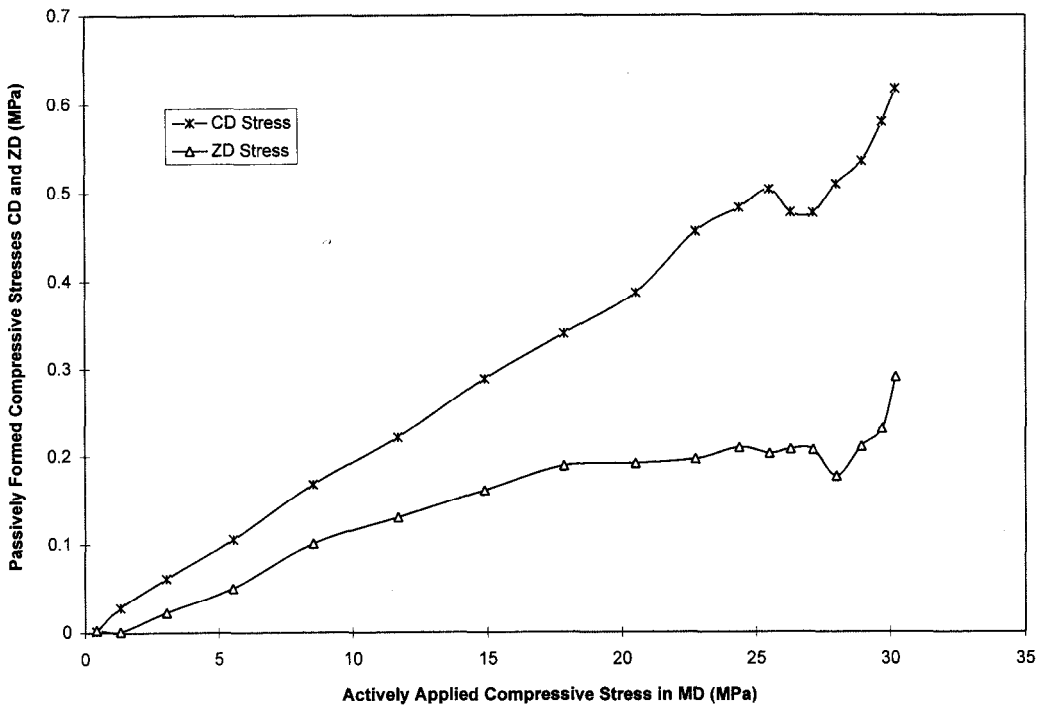

FIG. 5—*Comparison of stresses for paperboard cube actively loaded in MD.*

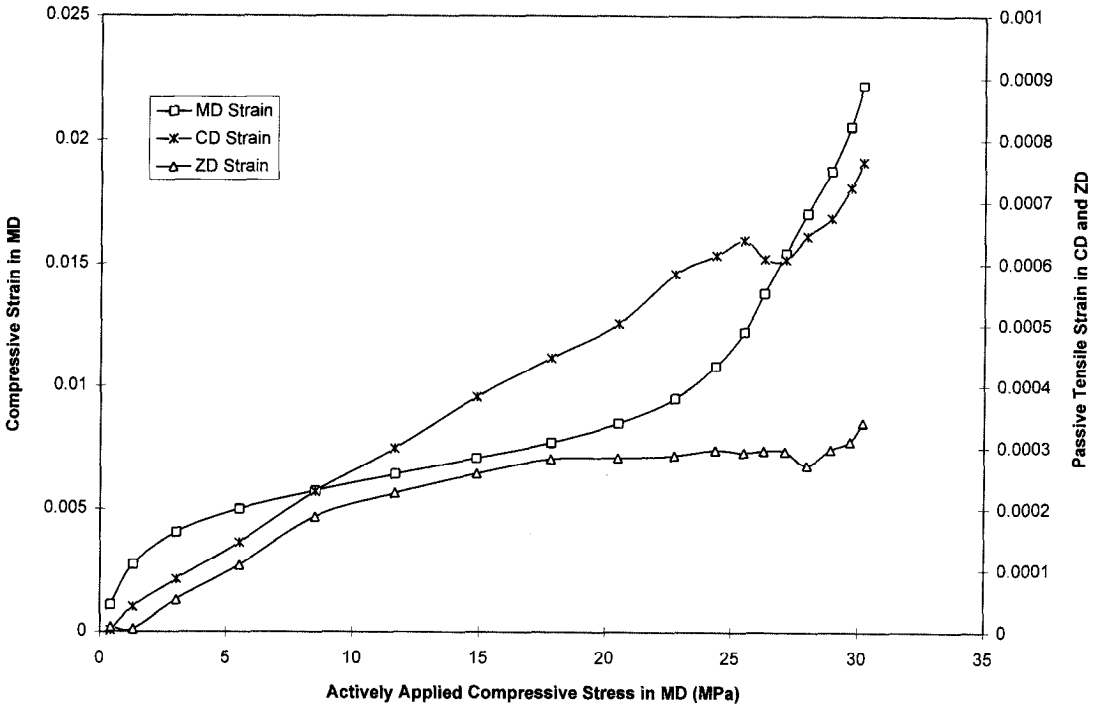

FIG. 6—*Comparison of strains for paperboard cube actively loaded in MD.*

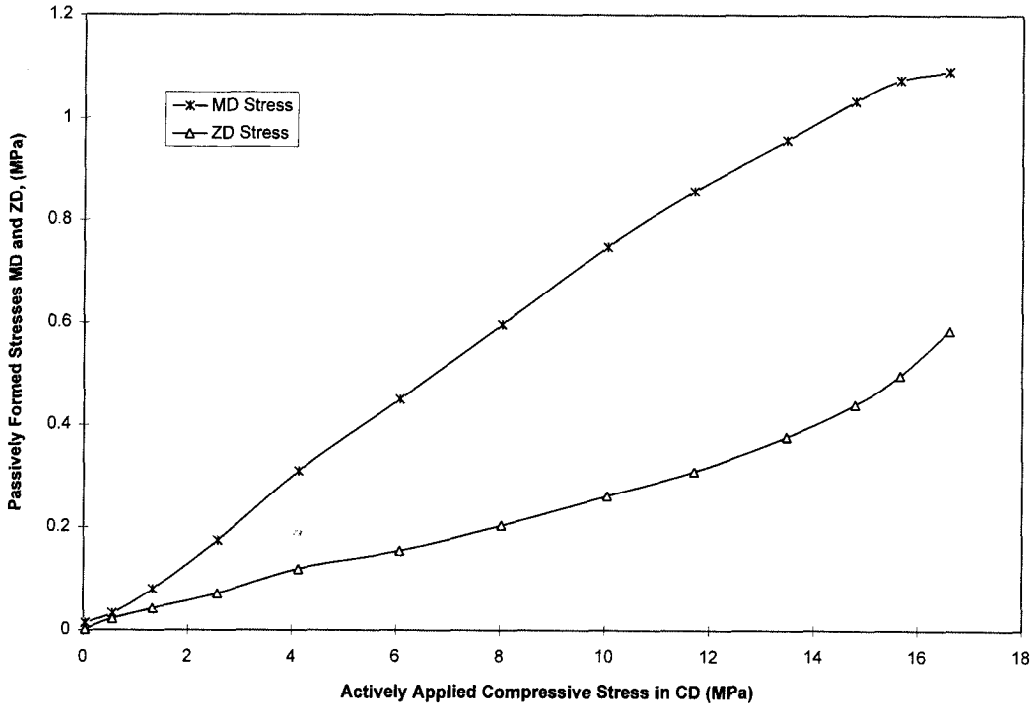

FIG. 7—*Comparison of stresses for paperboard cube actively loaded in CD.*

in the MD direction. The same pattern of data representation is repeated for the redwood specimens in Figs. 11 to 16.

These results show that measurable displacements and stresses were obtained along the three axes of investigation. Thus, the concept of using a passive restraint system was shown to be useful. However, the challenge presented by such data is to properly infer what strains may be present in totally arbitrary stress states. Attempts at such have begun [*12*], and further work is still needed in this area. The data shown here can provide a starting point for more general triaxial constitutive models.

Although it is not meaningful to directly compare the paperboard data (Figs. 5 to 10) to the redwood data (Figs. 11 to 16)

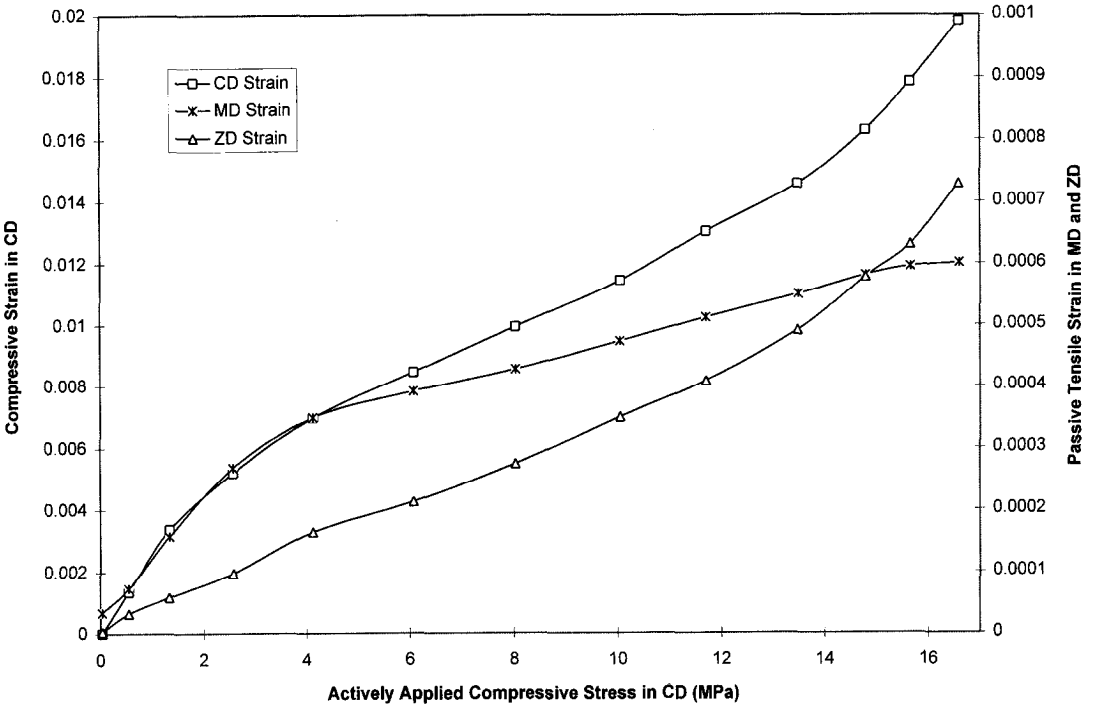

FIG. 8—*Comparison of strains for paperboard cube actively loaded in CD.*

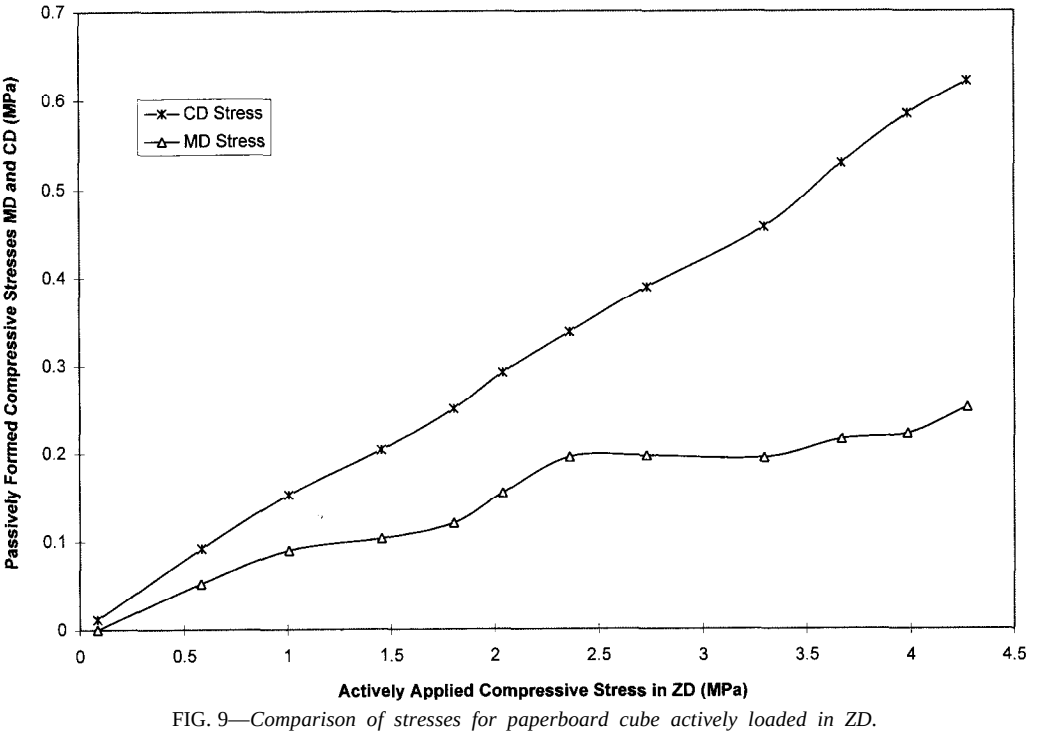

FIG. 9—*Comparison of stresses for paperboard cube actively loaded in ZD.*

differences in the data may highlight differences in designs for the devices. Comparing the levels of transverse stresses (Figs. 5 and 11) for cubes loaded in their strongest direction (MD and L), note that the redwood device was able to build up substantially greater transverse stresses. There are two possible explanations for this. First, the large amount of crush in the active direction for the redwood specimens forced greater transverse stresses to accumulate. Second, the improved platen positioning system of the second device created a more exacting fit around the specimen, resulting in an immediate and consequently greater buildup of transverse stresses.

A second observation drawn from comparing the two sets of

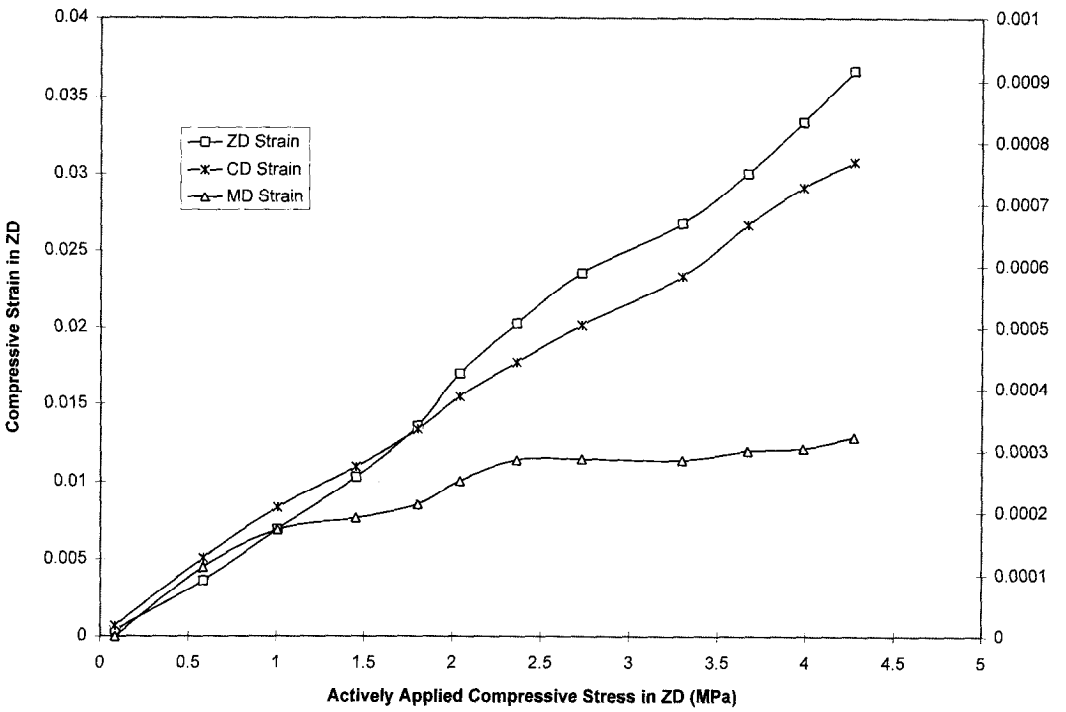

FIG. 10—*Comparison of* strains *for paperboard cube actively loaded in ZD.*

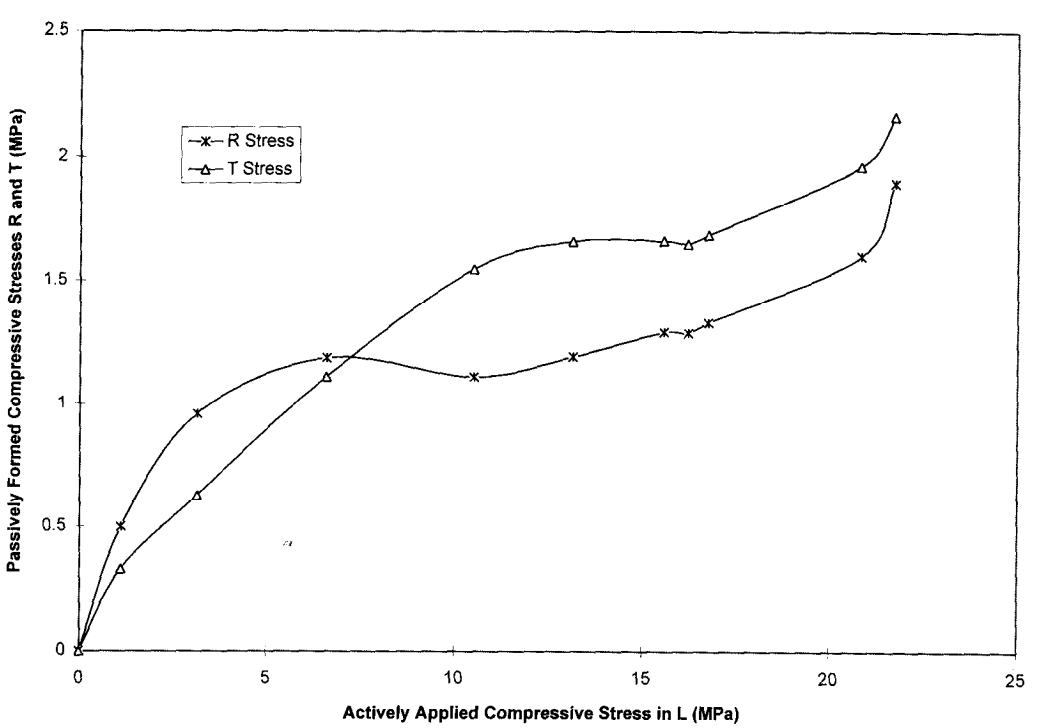

FIG. 11—*Comparison of stresses for redwood cube actively loaded in L.*

data (paperboard and redwood) is that the states of transverse strain are generally greater in the redwood device than in the paperboard device. Obviously, a part of the increase can be attributed to the greater transverse stresses, which we just discussed. Differing Poisson ratios can also account for some differences in measured magnitude of transverse strains. Nevertheless, it appears that the redwood testing device registers higher strains, even when states of transverse stress are comparable (see ZD stress and strain in Figs. 7 and 8, and compare with R stress and strain in Figs. 13 and 14). Thus, it is possible that the transverse strain data-collecting system was more sensitive in the redwood testing device than in the paperboard testing device.

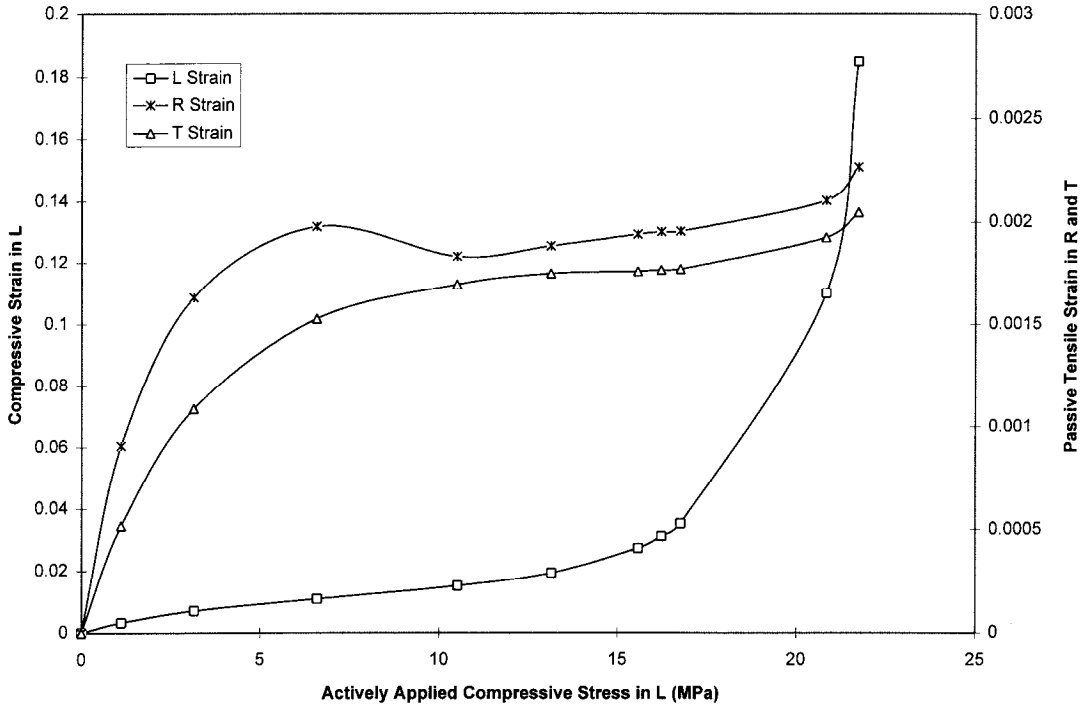

FIG. 12—*Comparison of strains for redwood cube actively loaded in L.*

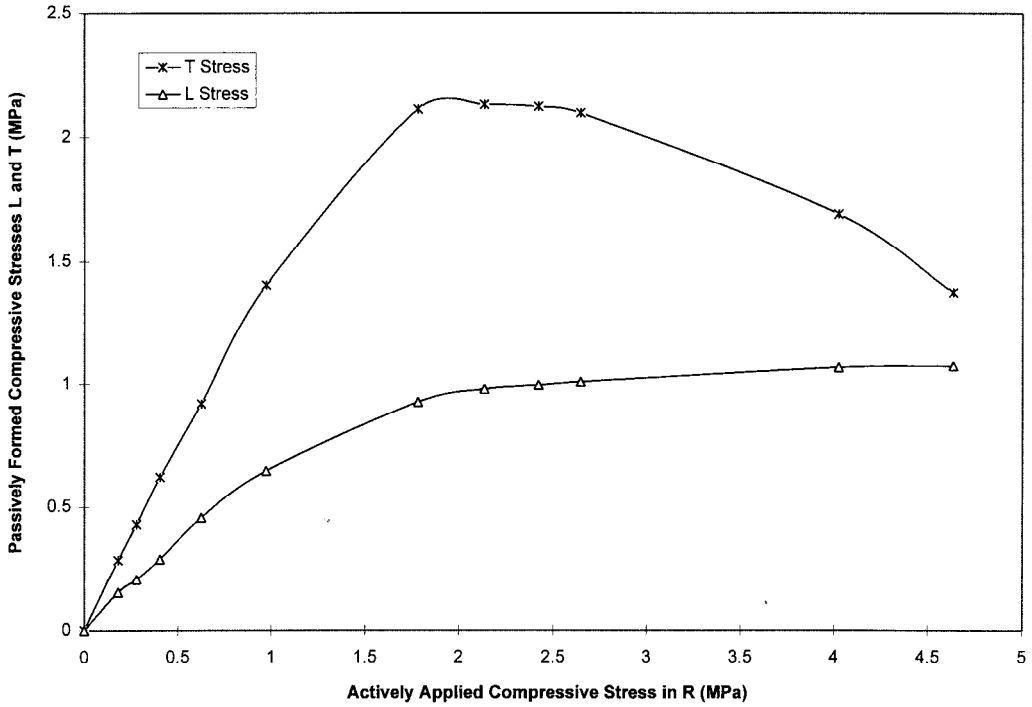

FIG. 13—*Comparison of stresses for redwood cube actvely loaded in R.*

Conclusions

As computational mechanics tools become more sophisticated, the need to accurately define the force deformation relationships of solids becomes more and more acute. This is particularly true of paperboard and wood, two orthotropic materials that have not been tested triaxially heretofore. As packaging and container designs become increasingly complicated, attempts to optimize and more rationally engineer these products will be hampered without progress in triaxial material testing.

Furthermore, constitutive models for orthotropic materials are rarely verified under triaxial stress states, even though such stress

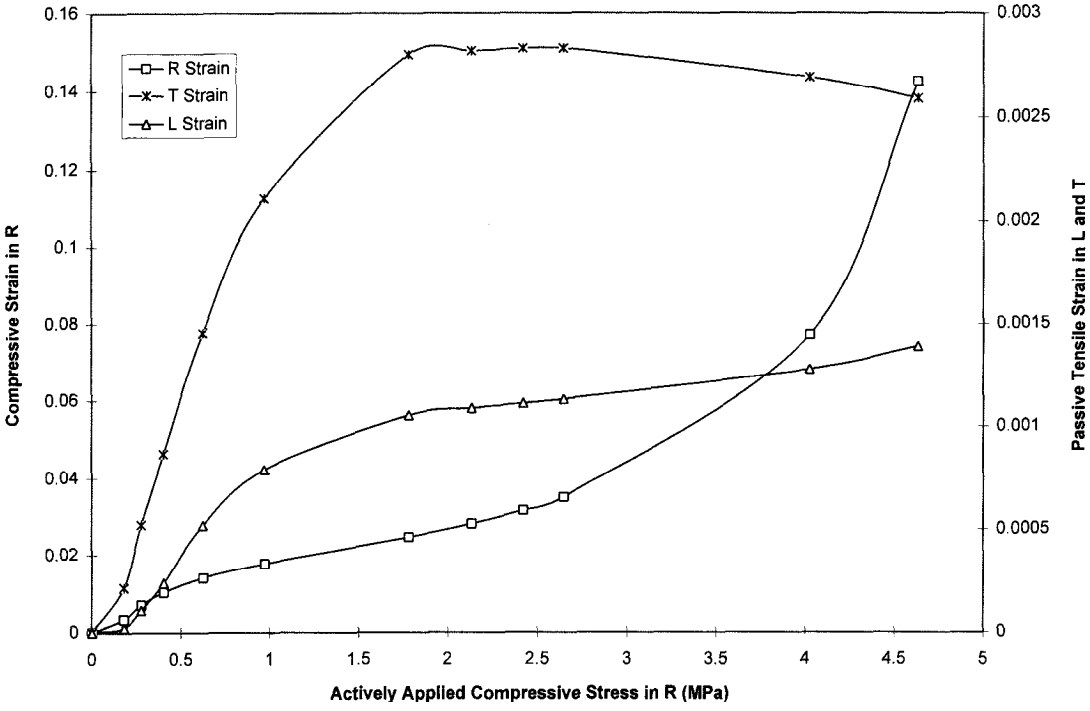

FIG. 14—*Comparison of strains for redwood cube actively loaded in R.*

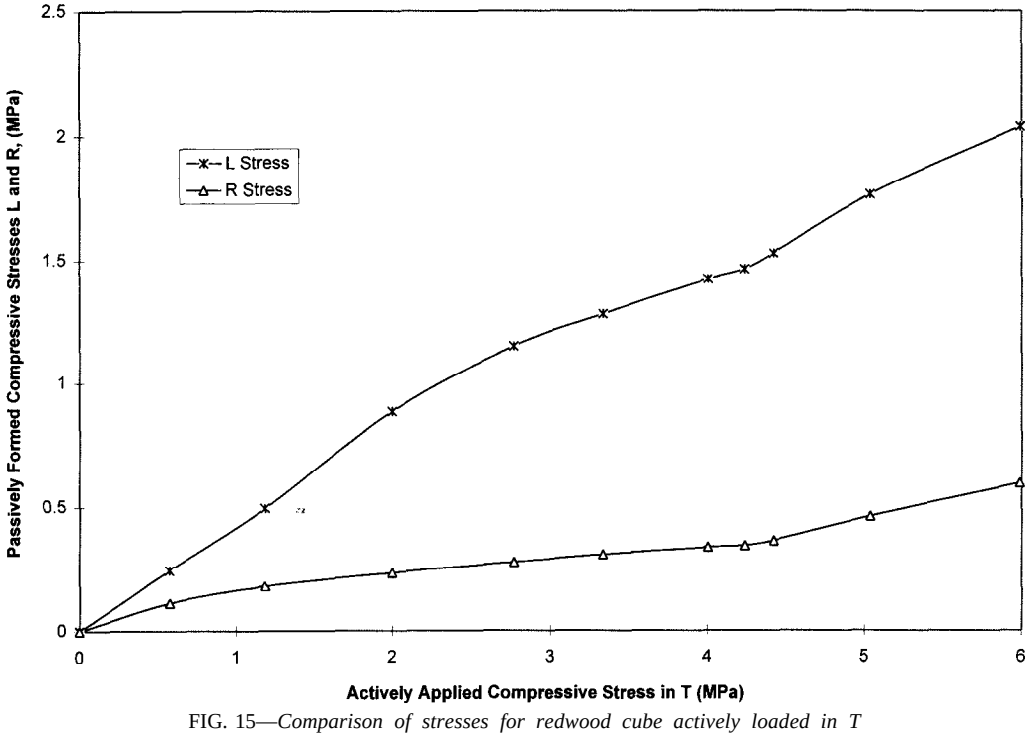

FIG. 15—*Comparison of stresses for redwood cube actively loaded in T*

conditions commonly occur in structural applications. Two economical devices for measuring triaxial material response are presented in this report. However, the inherent limitations of the fundamental design, a passive restraint system, needed to be quantified and overcome. The greatest difficulty with such a testing system is the quantification of surface effects. We conclude that surface-to-surface specimen strains can be much greater than strains at a central portion of the material. We identified two such effects: a buildup of frictional forces at the specimen-loading platen interfaces and local crushing of specimen asperities at this interface. Both of these effects clearly result in a nonuniform stress-strain condition in the specimen; therefore, each can cause the analyst to misinterpret

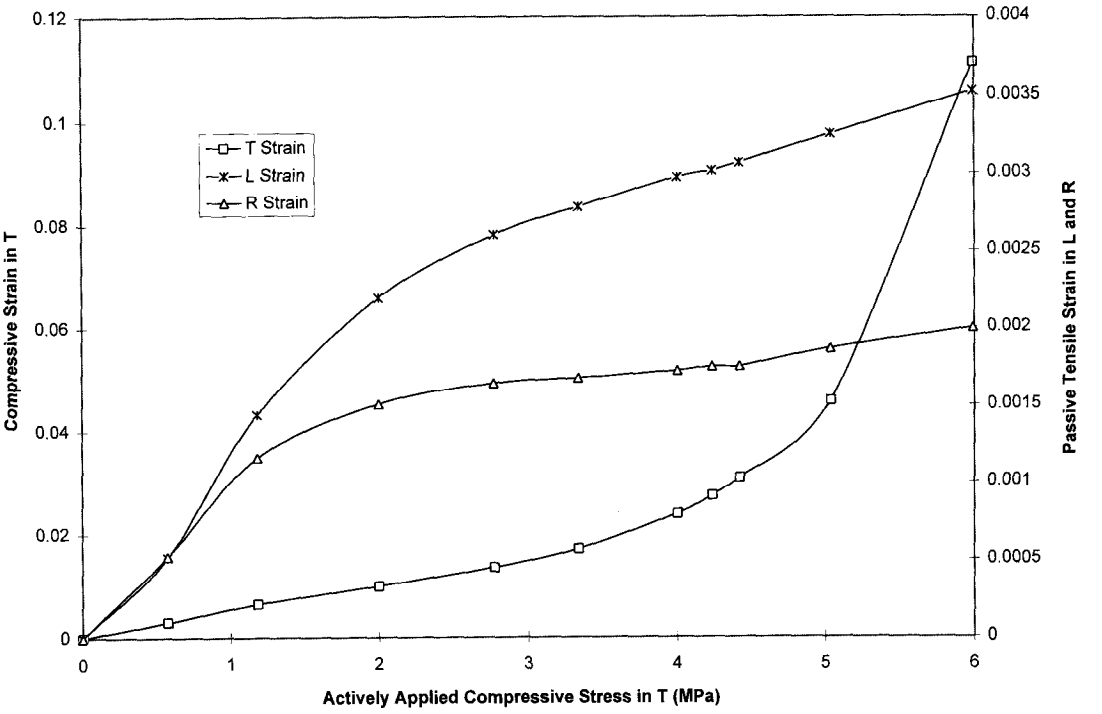

FIG. 16—*Comparison of strains for redwood cube actively loaded in T.*

the material moduli calculated from loading platen movement alone. Our approaches to quantify the surface effects included finite element analysis, calibrations with known materials, and supplementary uniaxial tests. We recommend that several such approaches be pursued to define these effects more fully. We also recommend further investigation into the role of friction in such testing devices. Our analysis of the data indicates that frictional forces impose shear stresses on the specimen. Finally, although the experimentally obtained triaxial load-deflection information was heavily influenced by surface effects and the modification processes may have been imperfect, the resulting reduced data are a practical body of information nevertheless. The paucity of such data highlights the need for more accurate representation of the true triaxial mechanical behavior of the orthotropic material being investigated. The use of the techniques proposed here reveals new information on the triaxial performance of orthotropic materials.

Acknowledgments

The authors gratefully acknowledge the support of Sonoco Products Corporation and Sandia National Laboratory.

References

[1] Johnson, M. W. and Urbanik, T. J., "A Nonlinear Theory for Elastic Plates with Applications to Characterizing Paper Properties," *Journal of Applied Mechanics,* Vol. 51, No. 3, 1984, pp. 145–152.

[2] Johnson, M. W. and Urbanik, T. J., "Buckling of Axially Loaded Long Rectangular Paperboard Plates," *Wood and Fiber Science,* Vol. 19, No. 2, 1987, pp. 135–146.

[3] Patton-Mallory, M., Cramer, S., Smith, F., and Pellicane, P., "Nonlinear Material Models for Analysis of Bolted Wood Connections," *Journal of Structural Engineering,* Vol. 123, No. 8, 1997, pp. 1054–1062.

[4] Suhling, J. C., "Constitutive Relations and Failure Predictions for Nonlinear Orthotropic Media," Ph.D. dissertation, Department of Engineering Mechanics, University of Wisconsin, Madison, 1985.

[5] Gerhardt, T. D., "External Pressure Loading of Spiral Paper Tubes: Theory and Experiment," *ASME Journal of Engineering Material and Technology,* Vol. 112, No. 4, 1990, pp. 144–150.

[6] Goodman, J. R. and Bodig, J., "Orthotropic Elastic Properties of Wood," *ASCE Journal of the Structural Division,* Vol. 96, St. 11, 1970, pp. 2301–2314.

[7] Sliker, A., Yu, Y., Weigel, T., and Zhang, W., "Orthotropic Elastic Constants for Eastern Hardwood Species," *Wood and Fiber Science,* Vol. 26, No. 1, 1994, pp. 107–121.

[8] *Test Method for Determining the Mechanical Properties of Hardened Concrete Under Triaxial Loads* (C 801), American Society for Testing and Materials, 1994.

[9] Wolcott, M. P., Kasal, B., Kamke, F. A., and Dillard, D. A. "Testing Small Wood Specimens in Transverse Compression," *Wood and Fiber Science,* Vol. 21, No. 3, 1989, pp. 320–329.

[10] *Practice for Force Verification of Testing Machines* (E 4) American Society for Testing and Materials, 1994.

[11] Cramer, S. M., Hermanson, J., and McMurtry, W. M., "Crush Performance of Redwood for Developing Design Procedures for Impact Limiters," *Proceedings,* Eleventh International Conference on Packaging and Transportation of Radioactive Materials, Las Vegas, NV, 1995.

[12] Saliklis, E. P., "A Nonlinear Constitutive Model for Paperboard," Ph.D. dissertation, Department of Civil and Environmental Engineering, University of Wisconsin, Madison, 1992.